Structural and Magnetic Properties of *A*-Site-Ordered Perovskites $ACu_3Sn_4O_{12}$ with $A = Ca^{2+}$, Sr^{2+}, and Pb^{2+}

Hiroshi Shiraki, Takashi Saito, and Yuichi Shimakawa*

Institute for Chemical Research, Kyoto University, Uji, Kyoto 611-0011, Japan

Received August 1, 2008. Revised Manuscript Received October 7, 2008

A series of *A*-site-ordered perovskites $ACu_3Sn_4O_{12}$ with $A = Ca^{2+}$, Sr^{2+}, and Pb^{2+} were prepared under high-temperature and high-pressure conditions. They have Cu^{2+} ions with $S = 1/2$ spins at the *A* site in the ABO_3 perovskite structure and have nonmagnetic Sn^{4+} ions at the *B* sites. An increase in the size of the divalent *A*-site ions from Ca to Pb increases the cubic lattice constant by only 0.6%. The cubic lattice with rigid CuO_4 units thus hardly expands and the different sizes of the *A*-site ions are accommodated by change of the SnO_6 octahedra. The difference in the size of the *A*-site ions has little effect on the ferromagnetic transition temperatures, because the magnetic properties of these perovskites are determined primarily by the direct ferromagnetic interaction between Cu^{2+} ions at the *A* site.

Introduction

Most copper oxides are antiferromagnets because the significant overlap between Cu 3d and O 2p orbitals usually causes antiferromagnetic superexchange interactions in Cu−O−Cu bonds to be dominant in such oxides.[1] On the other hand, a few cuprates are ferromagnetic. $SeCuO_3$ is an example, where the small Se^{4+} ion at the *A* site distorts the Cu−O−Cu bond angle into a range that according to the Kanamori−Goodenough rules makes this ABO_3-type perovskite structure ferromagnetic.[2,3] $La_4Ba_2Cu_2O_{10}$ is another ferromagnetic cuprate with a transition temperature of 5.2 K.[4] The square-coordinated CuO_4 units in this compound form a ladder-like structure along the *c* axis and they align perpendicular to each other in the *ab* plane. Although a few mechanisms such as a flat band model and a Hubbard model were proposed to explain the ferromagnetic property, none of them gave conclusive results.[5,6] Tajiri and Inoue recently proposed a mechanism in which the ferromagnetism is due to the Cu−O−O−Cu superexchange interaction by Hund's coupling of spins of holes in oxygen ions along the *c* axis.[7]

We recently found two other ferromagnetic cuprates, $CaCu_3Ge_4O_{12}$ and $CaCu_3Sn_4O_{12}$,[8,9] which are cubic *A*-site-ordered perovskites in which *A* and Cu ions are ordered at the *A* site in ABO_3-type perovskites (Figure 1). Calcium ions occupy one-fourth of the *A*-site positions forming a body-centered lattice with a $2a \times 2a \times 2a$ unit cell (*a*, unit cell of a simple ABO_3 perovskite). Jahn−Teller-distorted Cu^{2+} ions form square-coordinated CuO_4 units aligned perpendicular to each other. Since the Ge^{4+} and Sn^{4+} at the *B* site are nonmagnetic ions, only Cu^{2+} ($S = 1/2$) spins at the *A* site contribute to the magnetic properties of the materials. The discriminative arrangement of the CuO_4 units does not induce normal antiferromagnetic superexchange interaction, and the direct exchange interaction between the Cu^{2+} spins gives rise to the ferromagnetic behaviors of the compounds.[8]

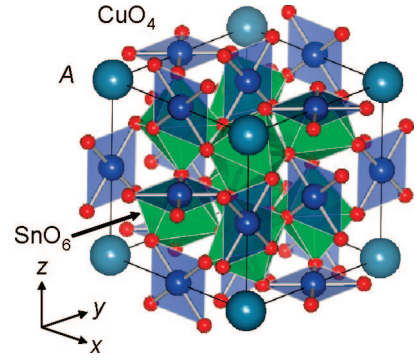

Figure 1. Crystal structure of $ACu_3B_4O_{12}$. The *A* ions (large spheres) and Cu ions (middle-size spheres) respectively occupy one-fourth and three-fourth of the *A*-sites of the ABO_3-type perovskite structure, and the *B*-site ions form corner-sharing BO_6 octahedra.

In this study we prepared a series of $ACu_3Sn_4O_{12}$ compounds with $A = Ca^{2+}$, Sr^{2+}, and Pb^{2+} and examined their structural and magnetic properties. The *A* site can accommodate these divalent ions with sizes ranging from small (Ca^{2+} with an ionic radius of 1.34 Å) to large (Pb^{2+} with an ionic radius of 1.49 Å), but the cubic lattice with rigid CuO_4 units hardly expands and structural adjustment is due to the distortion of the SnO_6 octahedra. As a result, the size of the *A*-site ion has little effect on the ferromagnetic direct exchange interaction and the ferromagnetic transition temperatures do not change much. A slight decrease in the ferromagnetic transition temperature of $PbCu_3Sn_4O_{12}$ appears

* To whom correspondence should be addressed. Tel: 81-774-38-3110. Fax: 81-774-38-3118. E-mail: shimak@scl.kyoto-u.ac.jp.

(1) See, for example, Goodenough, J. B. *Magnetism and the Chemical Bond*; Wiley: New York, 1963.
(2) Subramanian, M. A.; Ramirez, A. P.; Marshall, W. J. *Phys. Rev. Lett.* **1999**, *82*, 1558.
(3) Lawes, G.; Ramirez, A. P.; Varma, C. M.; Subramanian, M. A. *Phys. Rev. Lett.* **2003**, *91*, 257208.
(4) Mizuno, F.; Masuda, H.; Hirabayashi, I.; Tanaka, S.; Hasegawa, M.; Mizutani, U. *Nature* **1990**, *345*, 788.
(5) Eyert, V.; Hock, K. -H.; Riseborough, P. S. *Europhys. Lett.* **1995**, *31*, 385.
(6) Feldkemper, S.; Weber, W.; Schulenburg, J.; Richter, J. *Phys. Rev. B* **1995**, *52*, 313.
(7) Tajiri, S.; Inoue, J. *Phys. Rev. B* **2006**, *73*, 092411.

10.1021/cm8021209 CCC: $40.75
Published on Web 11/01/2008

to be caused by the antiferromagnetic interaction induced by hybridization of Pb 6s and O 2p orbitals.

Experimental Section

Polycrystalline samples of $ACu_3Sn_4O_{12}$ ($A = Ca^{2+}$, Sr^{2+}, and Pb^{2+}) were prepared under high-temperature and high-pressure conditions. $CaCO_3$, $SrCO_3$, PbO, CuO, and SnO_2 were used as starting powder materials for the synthesis. Calcined samples of $CaCu_3Sn_4O_{12}$ and $SrCu_3Sn_4O_{12}$ were made by heating the mixture of raw materials at 1000 °C for 20 h in air. They were ground, packed into gold capsules, and then pressed under 6 GPa at 1000 °C for 30 min with a cubic-anvil-type high-pressure apparatus. The mixture of PbO, CuO, and SnO_2 for the synthesis of $PbCu_3Sn_4O_{12}$ was treated under the same high-temperature and high-pressure condition used in the synthesis of $CaCu_3Sn_4O_{12}$ and $SrCu_3Sn_4O_{12}$.

Phase identification and crystal structure analysis of the resultant samples were carried out by synchrotron X-ray powder diffraction. Diffraction data at room temperature were collected with a large Debye−Scherrer camera installed at BL02B2 in the SPring-8 facility. Each sample was packed into a capillary 0.1 mm in diameter and was rotated during the measurement to minimize the influence of the preferred orientation on the diffraction pattern. The wavelengths λ used for the measurements were 0.77710 Å for $CaCu_3Sn_4O_{12}$ and $SrCu_3Sn_4O_{12}$, and 0.77336 Å for $PbCu_3Sn_4O_{12}$. The patterns obtained were fitted and the crystal structures were refined, by a Rietveld method, using the program RIETAN-2000.[10] Through the high energy of synchrotron X-ray and the use of the fine and thin capillary, absorption correction was not necessary for the analysis.

Magnetic properties of the samples were measured with a superconducting quantum interference device magnetometer (Quantum Design MPMS). Magnetic susceptibility was measured under an external magnetic field of 1 kOe at temperatures ranging from 5 to 300 K, and the magnetization at 5 K was measured under fields between −10 and 10 kOe. Specific heat at temperatures ranging from 2 to 50 K was measured, with a conventional relaxation method, using PPMS equipment (Quantum Design).

Results and Discussion

All the compounds synthesized were crystallized with the *A*-site-ordered perovskite structures. Even though the samples contained small amounts of impurities such as SnO_2 and CuO, the synchrotron X-ray powder diffraction patterns for the compounds were well fitted with an $Im\bar{3}$ *A*-site-ordered perovskite structure model. The refined structural parameters together with 12-coordinated Shannon's ionic radii[11] are summarized in Table 1, and an example of the Rietveld refinement pattern for $SrCu_3Sn_4O_{12}$ is shown in Figure 2.

It should be noted that as the size of the *A*-site cation in this series of compounds increases by about 11.2%, the cubic lattice constant increases by only 0.6%. In a simple rigid-sphere ionic model, the change in the size of the *A*-site ion from 1.34 Å for Ca^{2+} to 1.49 Å for Pb^{2+} leads to the change in the *A*-O bond distance from 2.74 to 2.89 Å by about 5.5% by assuming ionic radius for O^{2-} ion, r_O, of 1.4 Å. The corresponding cubic perovskite lattice, $(\sqrt{2})(r_A + r_O)$, should thus change by 5.5%. Even considering the *A*-site ions occupy one-fourth of the *A* site in a simple perovskite structure, about 1.4% of the lattice expansion is expected. However, the *A*−O bond distance increases by about 2.6% from 2.676 Å for Ca−O to 2.746 Å for Pb−O, which is much smaller than the expected change. Nor do that the lattice constants change much. All these observations imply that the size effect at the *A* site cannot be explained by a simple rigid-sphere ionic model and that the cage structure at the *A* site can accommodate ions of different sizes without significant structural change. The observed little change in the Cu−O distances also suggests a rigid structural framework with this special alignment of CuO_4. Although the Sn−O bond distance changes little (by only about 0.6%) when the *A*-site ion changes from Ca to Pb, the angle of the O−Sn−O bond in the SnO_6 octahedron changes significantly (increasing by 2.4%), reflecting the change of the octahedra.

Table 1. Refined Structural Parameters of $ACu_3Sn_4O_{12}$ ($A = Ca^{2+}$, Sr^{2+}, and Pb^{2+})[a]

	$CaCu_3Sn_4O_{12}$	$SrCu_3Sn_4O_{12}$	$PbCu_3Sn_4O_{12}$	Δ (%)
r_A (Å)	1.34	1.44	1.49	11.2
$r_A + r_O$ (Å)	2.74	2.84	2.89	5.5
a (Å)	7.64240(8)	7.67613(1)	7.69053(1)	0.6
x (O)	0.3050(3)	0.3070(5)	0.3106(4)	
y (O)	0.1719(3)	0.1748(5)	0.1761(5)	
B (A-site) (Å^2)	1.00(7)	0.81(7)	0.62(2)	
B (Cu) (Å^2)	0.27(1)	0.28(2)	0.56(3)	
B (Sn) (Å^2)	0.128(4)	0.189(5)	0.23(1)	
B (O) (Å^2)	0.53(4)	0.47(4)	0.32(7)	
R_{wp} (%)	4.12	3.91	3.55	
R_I (%)	2.17	1.47	2.14	
S	1.18	1.07	1.37	
Cu−Cu (Å)	3.8212(1)	3.8381(1)	3.8453(1)	0.6
A−O (Å)	2.676(3)	2.712(5)	2.746(3)	2.6
Cu−O (Å)	1.987(2)	1.999(2)	1.989(3)	0.1
Sn−O (Å)	2.0453(7)	2.0512(8)	2.0584(12)	0.6
O−Sn−O (deg)	88.8(1)	89.8(2)	90.9(1)	2.4
	(91.2(1))	(90.2(2))	(89.1(1))	

[a] The atom positions are: *A* 2*e* (0, 0, 0), Cu 6*b* (0, 0.5, 0.5), Sn 8*c* (0.25, 0.25, 0.25), and O 24*g* (*x*, *y*, 0). Also listed the Shannon's ionic radius, r_A, for the 12-coordinated *A*-site ion. Δ value is given by [parameter ($PbCu_3Sn_4O_{12}$) − parameter ($CaCu_3Sn_4O_{12}$)]/parameter ($CaCu_3Sn_4O_{12}$).

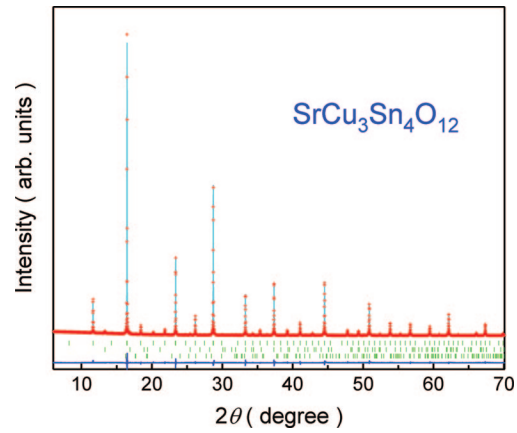

Figure 2. Synchrotron X-ray powder diffraction pattern and the result of Rietveld refinement for $SrCu_3Sn_4O_{12}$. Tick marks show the positions of allowed reflections from $SrCu_3Sn_4O_{12}$ (top), SnO_2 (middle), and CuO (bottom). Space group $Im\bar{3}$. $R_{wp} = 3.91\%$, $R_I = 1.47\%$, and $S = 1.07$.

(8) Shiraki, H.; Saito, T.; Yamada, T.; Tsujimoto, M.; Azuma, M.; Kurata, H.; Isoda, S.; Takano, M.; Shimakawa, Y. *Phys. Rev. B* **2007**, *76*, 140403(R).
(9) Shimakawa, Y.; Shiraki, H.; Saito, T. *J. Phys. Soc. Jpn.* **2008**, *77*, 113702.
(10) Izumi, F.; Ikeda, T. *Mater. Sci. Forum* **2000**, *321–324*, 198.
(11) Shannon, R. D. *Acta Crystallogr., Sect. A* **1976**, *32*, 751.

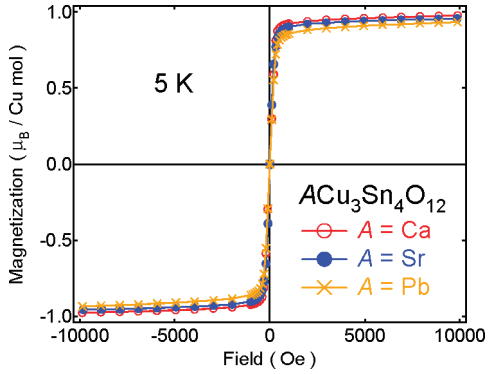

Figure 3. Magnetization of $ACu_3Sn_4O_{12}$ ($A = Ca^{2+}$, Sr^{2+}, and Pb^{2+}) at 5 K.

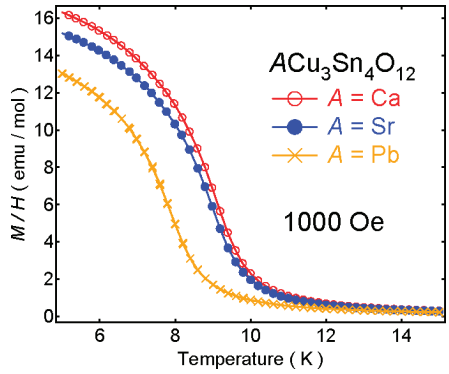

Figure 4. Temperature dependence of the magnetic susceptibility of $ACu_3Sn_4O_{12}$ ($A = Ca^{2+}$, Sr^{2+}, and Pb^{2+}).

It may also be worth mentioning that the crystal structure of the Pb^{2+}-containing $PbCu_3Sn_4O_{12}$ is cubic. Pb^{2+}-containing perovskites often show structural distortions like that seen in many ferroelectric oxides, and the distortion in $PbTiO_3$ is caused by the hybridization of Pb 6s and O 2p orbitals.[12] In $PbCu_3Sn_4O_{12}$, however, we do not see any macroscopic structural distortions from the cubic symmetry. This might be because in this compound the Pb^{2+} ions occupy only one-fourth of the *A* sites.

For each of the compounds we synthesized, magnetization is plotted in Figure 3 against the applied magnetic field. All the samples show ferromagnetic behaviors with saturation magnetization of about 1.0 μ_B/(Cu mol). Because the Sn^{4+} at the *B* site is nonmagnetic, the observed saturation magnetizations originate from the ferromagnetic alignment of Cu^{2+} ($S = 1/2$) spins at the *A* site. Figure 4 shows the temperature dependence of magnetic susceptibility. Sharp increases in the susceptibility at low temperature clearly indicate that ferromagnetic transitions occur. The transition temperatures of $CaCu_3Sn_4O_{12}$ and $SrCu_3Sn_4O_{12}$ are both ~10 K, whereas that of $PbCu_3Sn_4O_{12}$ is about 1 K lower. The magnetic susceptibility above the transition temperature of each compound obeys the Curie−Weiss law, and the Curie constant and the positive Weiss temperature are also consistent with ferromagnetic interaction between the localized Cu^{2+} ($S = 1/2$) spins.

A typical result of specific heat measurement is shown in Figure 5a, where the λ-type peak in the curve for $SrCu_3Sn_4O_{12}$ also confirms the second-order ferromagnetic

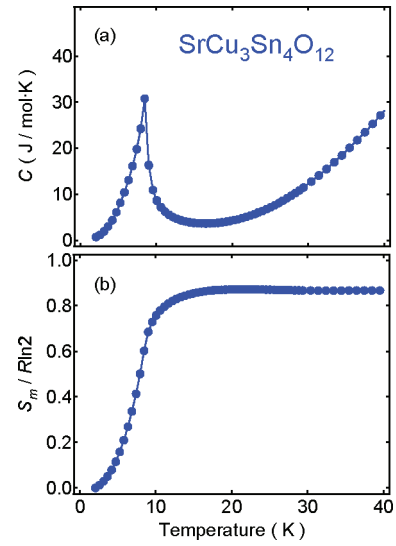

Figure 5. Temperature dependence of (a) specific heat of $SrCu_3Sn_4O_{12}$ and (b) the magnetic entropy to the full entropy with $S = 1/2$ spins (Rln 2).

transition. As shown in Figure 5b, the magnetic entropy estimated by subtracting the Debye's T^3 lattice contribution in the $C(T)/T$ plots, i.e., $S_m = \int (C_m/T)\,dT$, accounts for more than 80% of the total entropy of an $S = 1/2$ spin system (Rln 2) This implies that long-range-ordered magnetic structure is well established in the vicinity of the transition temperature. Similar results were also obtained when the specific heat of $CaCu_3Sn_4O_{12}$ and $PbCu_3Sn_4O_{12}$ were measured, and the transition temperatures agree well with those observed in the magnetic measurements.

As we discussed in previous papers, the special alignment of the square-coordinated CuO_4 units in the *A*-site-ordered structure does not induce normal antiferromagnetic superexchange interaction between the Cu^{2+} spins through the oxygen ions but does induce the ferromagnetic direct exchange interaction.[8,9] This explains the ferromagnetic behaviors in the present $ACu_3Sn_4O_{12}$ ($A = Ca^{2+}$, Sr^{2+}, and Pb^{2+}) system. Despite the different sizes of the Ca^{2+}, Sr^{2+}, and Pb^{2+} ions, the Cu−Cu distances (half of the lattice constant) of $CaCu_3Sn_4O_{12}$, $SrCu_3Sn_4O_{12}$, and $PbCu_3Sn_4O_{12}$ do not differ much. As a result, the size of the *A*-site ion has little effect on the ferromagnetic direct exchange interaction, and the transition temperatures of $CaCu_3Sn_4O_{12}$ and $SrCu_3Sn_4O_{12}$ should be quite similar. The transition temperature of $PbCu_3Sn_4O_{12}$, on the other hand, is slightly lower than those of $CaCu_3Sn_4O_{12}$ and $SrCu_3Sn_4O_{12}$. The Pb^{2+} ion has a lone pair of electrons in the 6s orbital and that orbital often hybridizes with O 2p near the Fermi level. Thus, the hybridization of Pb 6s and O 2p may induce antiferromagnetic superexchange interaction through Cu−O−Pb−O-Cu and reduce the ferromagnetic transition temperature slightly.

Conclusions

We prepared a series of *A*-site-ordered perovskites $ACu_3Sn_4O_{12}$ with $A = Ca^{2+}$, Sr^{2+}, and Pb^{2+}. All samples show long-range ordered ferromagnetic behaviors with Cu^{2+} ($S = 1/2$) spins. As the size of the *A*-site cation increases from Ca^{2+} to Sr^{2+} to Pb^{2+}, the cubic lattice constant

increases by only 0.6%. The cubic lattice thus hardly expands, and the different sizes of the *A* site ions are accommodated by distortion of the SnO_6 octahedra. Because the Cu−Cu distances show no significant variation, the ferromagnetic transition temperatures for all compounds are quite similar. The results are consistent with the ferromagnetic interaction in $ACu_3Sn_4O_{12}$ being primarily a result of the direct ferromagnetic interaction between Cu^{2+} spins at the *A* site. The slightly lower ferromagnetic transition temperature of $PbCu_3Sn_4O_{12}$ might be a result of the hybridization of Pb 6s and O 2p orbitals, which induces antiferromagnetic superexchange interaction through Cu−O−Pb−O−Cu.

Acknowledgment. We thank M. Azuma for useful discussion. The synchrotron X-ray diffraction experiments were performed at SPring-8 with the approval of the Japan Synchrotron Radiation Research Institute. This work was partly supported by Grants-in-Aid for Scientific Research (19GS0207, 18350097, 17038014, and 17105002) and by the Joint Project of Chemical Synthesis Core Research Institutions from the Ministry of Education, Culture, Sports, Science and Technology, Japan.

CM8021209

(12) Choen, R. E. *Nature* **1992**, *358*, 136.